Numerical Relativity and the Discovery of Gravitational Waves

Robert A. Eisenstein*

MIT LIGO, NW22-272, 185 Albany St., Cambridge, MA 02139
(Dated: April 23, 2018)

Solving Einstein's equations precisely for strong-field gravitational systems is essential to determining the full physics content of gravitational wave detections. Without these solutions it is not possible to extract precise values for initial and final-state system parameters. Obtaining these solutions requires extensive numerical simulations, as Einstein's equations governing these systems are much too difficult to solve analytically. These difficulties arise principally from the curved, non-linear nature of spacetime in general relativity. Developing the numerical capabilities needed to produce reliable, efficient calculations has required a Herculean 50-year effort involving hundreds of researchers using sophisticated physical insight, algorithm development, computational technique and computers that are a billion times more capable than they were in 1964 when computations were first attempted. My purpose is to give an accessible overview for non-experts of the major developments that have made such dramatic progress possible.

I. OVERVIEW OF A BLACK-HOLE BLACK-HOLE COALESCENCE

On September 14, 2015, at 09:50:45 UTC the two detectors of the advanced Laser Interferometer Gravitational-Wave Observatory (aLIGO)[1] simultaneously observed[2] the binary black hole merger known as GW150914. The binary pair merged at a luminosity distance of 410^{+160}_{-180} Mpc. Analysis revealed[3] that the two BH masses involved in the coalescence were, in the source frame, $35.8^{+5.3}_{-3.9}$ and $29.1^{+3.8}_{-4.3}$ $M_\odot$, while the mass of the final-state BH was $62.0^{+4.1}_{-3.7}$ $M_\odot$. The difference in mass between the initial and final state, $3.0^{+0.5}_{-0.4}$ $M_\odot$, was radiated away as gravitational radiation. No associated electromagnetic radiation or other cosmic rays were observed. Astonishingly, the coalescence and ringdown to a final stable BH took less than 0.2 second (within LIGO's frequency band), coming after an orbital dance lasting billions of years. This observation, coming 100 years after Einstein's publication of general relativity, is yet another confirmation of its validity. It also is the first direct confirmation that BHs can come in pairs.

Figure 1 is a comparison of the observed strains at the Hanford and Livingston LIGO sites after shifting and inverting the Hanford data to account for the difference in arrival time and the relative orientation of the detectors. The event was identified nearly in real time using detection techniques that made minimal assumptions[4] about the nature of the incoming wave. Subsequent analysis used matched-filter techniques[5] to establish the statistical significance of the observation. Detailed statistical analyses using Bayesian methods were used to estimate the parameters of the coalescing BH–BH system.[3]

Long before coalescence occurs, the two orbiting BHs can be represented as point masses co-rotating in an orbit of very large size. This "inspiral" is indicated on the left side of Fig. 2. As the inspiral progresses, the orbit becomes circularized due to energy loss. The spacetime is basically flat except near each BH. Even so, Newtonian physics cannot accurately describe what is happening.
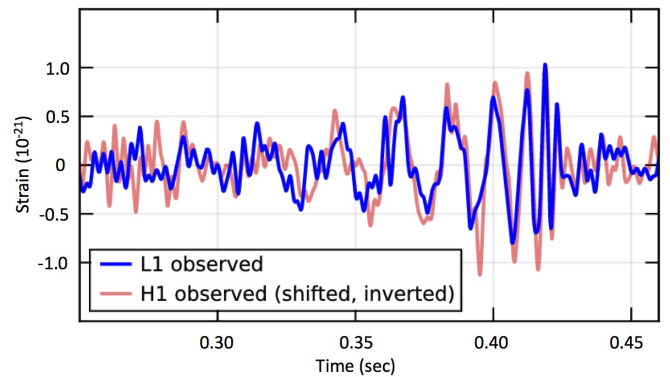

FIG. 1. GW strains within a 35–350 Hz passband measured at the Hanford and Livingston LIGO observatories during the detection of GW150914. Time is measured relative to 09:50:45 UTC. The event arrived $6.9^{+0.5}_{-0.4}$ ms later at Hanford than at Livingston (see text). (From Ref. 2)

Instead, "Post-Newtonian" (PN)[6] and "Effective One-Body" (EOB)[7] methods must be employed.

As the BH's near each other (center, Fig. 2), spacetime begins to warp significantly and the BH horizons are distorted. The EOB approach provides a good description (better than one might expect) until the beginning of coalescence, when the spacetime becomes significantly curved and highly non-linear. In fact, the inspiraling waveform depends strongly on several aspects of the BH–BH interaction, *e.g.* their masses, spins, polarizations and orbit eccentricity. This dependence plays a key role in the extraction of those parameters, but requires fits to numerical relativity simulations to reproduce the correct result as the binary system approaches merger. Recently, parameter estimation methods have directly used numerical relativity simulations[8–10] to do this.

Soon after the BH's reach their "innermost stable circular orbit" (ISCO) they "plunge" together, coalescing into a single highly vibrating, spinning (Kerr)[11] BH. Numerical relativity is needed to describe this. The final BH rings down via the emission of gravitational radiation to
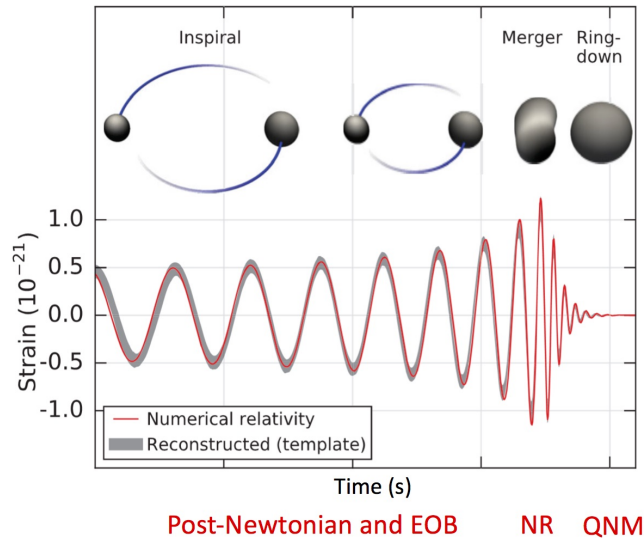
FIG. 2. Top: A schematic drawing of the inspiral, plunge, merger and ringdown of two coalescing BHs (see text). Bottom: Comparison of a best-fit template of the measured strain data to the predicted unfiltered theoretical waveform, calculated using the extracted physical parameters. (From Ref. 2)

a stable, spinning, non-radiating BH. The ringdown can be described using a perturbative quasi-normal modes model.[12] An overview of the basic physics of the entire BH–BH merger is available in Ref. 13.

II. EINSTEIN'S EQUATIONS

Einstein's equations,[14,15] written in final form in November, 1915, are expressed in terms of the four generalized coordinates of spacetime, which is represented as a geometrical *Riemann manifold*[16] $\mathcal{M}$ that extends to infinity in all directions.[17] Three of the coordinates (labeled 1-3) are spatial and one (labeled 0) represents time. At this stage, they are not represented by a specific coordinate system. The manifold shape is determined by the real 4-by-4 metric tensor $g_{\mu\nu}$, which in Einstein's theory is determined by the mass densities and energy fluxes present at every point in spacetime. These relationships are summarized by Einstein's equations written in tensor form:[18,19]

$$G_{\mu\nu} := R_{\mu\nu} - \frac{1}{2}g_{\mu\nu}R = 8\pi T_{\mu\nu} \qquad (1)$$

The quantity $G_{\mu\nu}$, Einstein's tensor,[20] is defined in terms of the metric tensor $g_{\mu\nu}$, the Ricci curvature tensor[21] $R_{\mu\nu}$ and the Ricci scalar[22] R. The energy-momentum, or stress-energy, tensor is represented by $T_{\mu\nu}$.

A remarkable feature of Einstein's equations is that the geometry of spacetime appears only on the left-hand side, imbedded in $G_{\mu\nu}$, while the physical momentum-energy content appears only on the right, imbedded in $T_{\mu\nu}$. Thus, as John Wheeler memorably remarked: "Matter tells spacetime how to curve, and spacetime tells matter how to move."

The metric tensor $g_{\mu\nu}$ plays the same role in general relativity as it does in special relativity. In each case it provides the link between the generalized coordinates x_μ and the invariant spacetime interval ds: $ds^2 = g_{\mu\nu}dx^\mu dx^\nu$, summing as usual over repeated indices. In special relativity it defines a flat (Minkowski)[23] space. In general relativity it defines the curved (Riemannian)[16] manifold $\mathcal{M}$. The curvature, due to gravitational sources, enters via the Ricci tensor $R_{\mu\nu}$ and the Ricci scalar R. Thus in both special and general relativity, the metric tensor elements determine all the physical observables we can calculate.

The subscripts (μ, ν) range over the integers 0 to 3, implying the need to solve a system of 16 coupled equations. However, the symmetries of the metric limit the actual number to 10. The simple appearance of Einstein's equations in tensor notation masks a very great deal of complexity. When written out in full they can contain thousands of terms. These will have significant non-linearities due to the spacetime curvature that occurs when the gravitational fields are very strong.

III. SOLVING EINSTEIN'S EQUATIONS

Due to the complexities mentioned above, there are very few analytical solutions of Einstein's equations of physical relevance. The ones we know of arise in situations involving a high degree of symmetry. Most important for the present discussion are the Schwarzschild solution[24] (for a spherically-symmetric mass M with spin 0) and the Kerr solution[11] (for a spherically-symmetric mass M with spin J). Exact solutions that include a charge Q on the BH (an unlikely prospect) have also been found but will not be discussed here.

Schwarzschild's 1916 discovery led to one of the most important predictions of general relativity: the existence of BH's. A valuable simplification comes in the form of the "no-hair" conjecture,[25] which states that in four dimensions the BH solutions to Einstein's equations can only depend on the mass, spin and charge of the BH.

Einstein predicted the existence of gravitational waves[26–28] moving at the speed of light[29] in 1916. Reasoning by analogy to electromagnetism (*i.e.* accelerating masses should radiate gravitational waves as accelerating charges radiate electromagnetic ones),[30] he found them by linearizing Einstein equations for the case of nearly flat spacetime (*i.e.* weak gravitation). For many years there was considerable uncertainty as to their existence, even from Einstein himself, but the issue was put to rest[31] in the mid-1950's. Gravitational waves exist in the strong field case also, but the equations describing them are not linear. It is those equations we must solve numerically in order to observe and quantify the nature of BH–BH,

BH–Neutron Star (NS) or NS–NS coalescences.

As if BHs and gravitational waves were not enough, Einstein's equations also predict that the structure of the Universe is not static: as time goes on, it will either expand or contract. Since there was no evidence in 1916 for either of these prospects, Einstein introduced a "cosmological constant" to force his equations to predict a static Universe. When the expansion of the Universe[32] was established in 1926, he later called this decision "my greatest blunder." Ironically, with the discovery[33] in 1998 that the Universe is accelerating as it expands, the cosmological constant plays an important role in accounting for (if not understanding) the cosmic acceleration.

IV. NUMERICAL RELATIVITY AND BH–BH COALESCENCE[34–38]

It is worth pointing out that even though these calculations are prodigiously difficult, the BH–BH system is very likely the simplest strongly–interacting gravitational problem we will ever encounter. If the study of strong-field general relativity is to have a future, it is imperative to solve it.

The long road to stable, convergent numerical solutions began in 1952, when Yvonne Fourès-Brouhat[39] showed that Einstein's equations were *well-posed*. Simply put, this means: (1) that solutions of the equations exist; and (2) that small changes to initial conditions produce only stable, continuous (*i.e.* non-chaotic) changes in the output. Given the difficulty of Einstein's equations, these seemingly reasonable expectations are far from obvious.

A. The ADM Procedure

During the next several decades, many substantial difficulties[40] had to be overcome to obtain stable, accurate solutions. The first was to recast Einstein's equations in the form of a computable, time-step iteration process (*i.e. an initial value problem*) that would evolve from initial conditions (*i.e.* an initial spacetime), through BH–BH coalescence, to the boundary conditions for the final state. In the world of partial differential equations (PDE's) this is called a *Cauchy problem*. In general relativity, this recipe is referred to as a "3+1" approach because space and time are separated. This formulation comes at a price: giving up overall covariance. It was first proposed by Arnowitt, Deser and Misner[41] (ADM) in 1962.

In 1979, York rewrote[42] the original ADM prescription to emphasize its role in evolving the Einstein equations[43] rather than as a basis for a theory of quantum gravity (the original intent of the ADM work). His treatment is now ubiquitously referred to as the "ADM" prescription. It has spawned many close cousins, all of which are referred to as "3+1" algorithms (see Sec. IV B).

The basic ADM idea is to decompose the spacetime by creating a stack of *3-dimensional, spacelike "foliations"*, or slices, each characterized by a fixed coordinate time (see Fig. 3). These we label Σ_t. The system evolves by moving with time from one foliation to the next. The invariant spacetime interval, formerly written as $ds^2 = g_{\mu\nu}dx^\mu dx^\nu$, becomes in the "3+1" description:

$$ds^2 = (-\alpha^2 + \beta^i\beta_i)dt^2 + 2\beta^i dtdx^i + \gamma_{ij}dx^i dx^j \quad (2)$$

Here the γ_{ij} are the *3-dimensional* metric tensors for these surfaces. The indices i and j run from 1 to 3. Note that time appears explicitly. The quantity α (the *lapse*) and the three β_i (the *shift vector* $\vec{\beta}$) are *gauge variables*[44] that may be freely specified but must be chosen with care. The *lapse* determines the rate at which one progresses perpendicularly from one slice to the next; it can be varied as the problem evolves. A lot of thought goes into choosing α because it determines the distance between the foliations; good choices avoid singularities. The *shift vector* basically measures how much the spatial coordinates change between foliations.

Because the foliations Σ_t are embedded in the overall spacetime manifold $\mathcal{M}$, they are characterized by the real *Extrinsic Curvature Tensor* K_{ij} that describes the nature of the embedding:[45]

$$\mathcal{K}_{ij} = \frac{1}{2\alpha}(\partial_t\gamma_{ij} - \mathcal{D}_i\beta_j - \mathcal{D}_j\beta_i) \quad (3)$$

Here the symbol ∂_t is an ordinary partial derivative with respect to time, and $\mathcal{D}_i$ is a spatial covariant derivative.

Evolving Einstein's equations using a "3+1" method requires that initial values of $g_{\mu\nu}$ and $\mathcal{K}_{ij}$, 12 numbers in all, must be fixed. But they cannot be chosen arbitrarily because of the *constraints* discussed in the next Section.
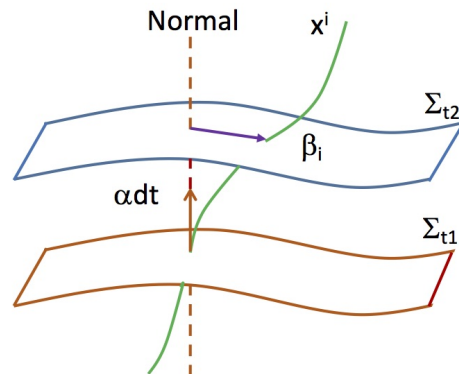

FIG. 3. A schematic 3+1 ADM decomposition. Σ_{t1} and Σ_{t2} are spacelike 3-dimensional foliations separated by coordinate time $t_2 - t_1$. The quantity $\alpha\,dt$, with α the *lapse*, is the time step between Σ_{t2} and Σ_{t1}. The *shift* β_i measures the change in coordinate x^i in moving from the earlier foliation.

Despite the promise of the ADM method, evolving a BH–BH system through coalescence remained elusive. The reason was that its equations are only *weakly hyperbolic* (see Sec. IV B and Ref. 46) and so are ill-posed.

B. ADM Evolution and Constraints

As mentioned in Sec. II, the symmetries of the metric tensor reduce Einstein's set of 16 equations for the $g_{\mu\nu}$ to 10 coupled, non-linear PDE's.

Evolution equations. Of the 10, six contain space and time derivatives up to second order. These equations provide the *evolution* of the initial spacetime. They contain mixtures of *hyperbolic* and *parabolic* (*i.e.* time-dependent) behavior. Hyperbolic equations are basically wave equations that describe wave propagation at finite speed. Solutions to wave equations are generally very stable and converge rapidly. Real parabolic equations (*e.g.* the heat equation) do not exhibit wave-like behavior. On the other hand, a parabolic equation with an imaginary component (*e.g.* the Schrödinger equation), exhibits both a wave speed and dispersion.[47]

Constraint equations. The remaining four equations have no time derivatives and serve as *constraints* on the time development. They are *elliptic* (*i.e.* time-independent) equations. These are often used to describe time-independent boundary-value problems. Because of the non-linearity of strong-field general relativity, they are harder than usual to solve numerically.

In theory, once the constraints are satisfied initially they should remain so. But for numerical solutions that is often not the case, especially when significant non-linearities are present. Small numerical errors can exponentially grow. Keeping the constraints satisfied at all times has proven essential to reaching stable, convergent solutions of the BH–BH coalescence problem.

An instructive parallel appears with Maxwell's equations. There, the laws of Ampère and Faraday, both containing time derivatives of the electric and magnetic fields $\mathbf{E}$ and $\mathbf{B}$, are the evolution equations, while Gauss's Laws for $\mathbf{E}$ and $\mathbf{B}$ serve as constraints. Since these equations are linear the constraints are usually well-behaved. When they aren't, the results are not solutions to Maxwell's equations. The analogue is true in numerical relativity.

For most rapid convergence the evolution equations should be as wave-like (hyperbolic) as possible. Gauge freedom is useful for this purpose, keeping in mind that poor gauge choices can adversely affect well-posedness. The constraint equations have proven very useful here. Since they can always be written in the form $\mathcal{C}(x, y, z) = 0$ (*e.g.* $\nabla \cdot \mathbf{E} - 4\pi\rho = 0$), one can add them (or multiples of them) to the evolution equations wherever that might be useful. Picking coordinates (a gauge choice) is also crucially important.

There are many other ways[48,49] to use gauge freedom to control problems arising from convergence issues, physical or coordinate singularities, numerical round-off error, and issues associated with boundary problems at BH horizons (among others). Perhaps the most important lesson in the development of numerical relativity is that gauge choices (including the choice of coordinates[50]) are every bit as important as computing power.

Especially important is the 1987 work of Nakamura, Oohara and Kajima, which presented[51] a version of ADM that showed much better stability. Later, Shibata and Nakamura[52] (1995) and Baumgarte and Shapiro[53] (1998) confirmed and extended those results. These efforts are commonly known as the *BSSNOK approach*.[54] It was essential to achieving full 3-dimensional simulations of BH–BH coalescences and is in wide use today. It confirms the importance of selecting carefully the best formulation of Einstein's equations for the problem at hand.

C. Harmonic Coordinates and Constraint Damping

Beginning with Einstein, harmonic coordinates have played a major role in general relativity.[55] As noted in Sec. IV, they were used by Fourès-Brouhat[39] to show the well-posedness of Einstein's vacuum equations. Today, in a *generalized form*,[55,56] they are important in solving numerically the BBH coalescence problem.[57] They work well because they convert Einstein's equations into second-order strongly hyperbolic form. The ADM formulation, with redefinitions of the lapse and shift, can accommodate them as well. The same cautions about constraint damping apply. We refer to this overall approach,[57] Generalized Harmonics with Constraint Damping, as GHCD.

D. Initial Conditions

In the BSSNOK approach, the initial data consist of values for the γ_{ij} metric and the extrinsic curvature matrix $\mathcal{K}_{ij}$. These depend on the initial parameters of the BH's or NS's, and on the gauge variables α and $\vec{\beta}$. As mentioned earlier, these cannot all be chosen independently because of the constraint equations, which in addition are hard to solve numerically. This difficult problem has been studied extensively.[58–61] In the GCHD treatment, initial values for the four spacetime coordinates and their first derivatives are specified. In both approaches the initial constraints are imposed and then enforced throughout the calculation.

E. Excisions and Moving Punctures

We are dealing with simple Schwarzschild or Kerr BHs having event horizons behind which the singularites are hidden from view (an idea known as *cosmic censorship*[62]). It led William Unruh[63] to suggest in 1984 that BH singularities could be *excised* from the calculation so that their influence is never felt outside the horizon. Thus information can flow into, but not out of, a BH. Fig. 4 shows the imminent coalescence of two non-equal BH's viewed from this perspective. Note the numerical boundary just below the BH horizon.

However, excision comes at the expense of very demanding boundary conditions. The BH horizons are continuously moving and spurious numerical artifacts can

arise (including the unphysical emission of gravitational radiation), making fine-tuning the calculation and enforcement of the constraints a continuous necessity.
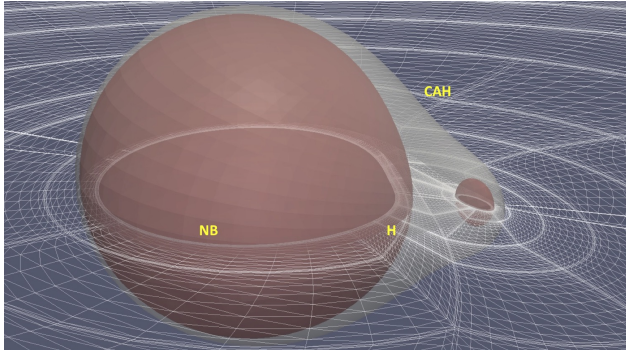

FIG. 4. A body-shaped, two-center coordinate system for unequal mass BHs. "H" labels a BH horizon while "NB" is its numerical boundary. No mesh is needed beneath that surface. "CAH" is the common apparent horizon. At far distances the coordinate lines are close to spherically symmetric. (From M. Scheel, used with permission)

Another approach is to view BHs as Einstein-Rosen bridges[64] (See Fig. 5). This was done first by Hahn and Lindquist[65] in their seminal 1964 calculations of BH–BH coalescence that founded numerical relativity.[66] The singularity lies on the wormhole axis perpendicular to the spacetimes that are above and below. Note that the coordinate lines can approach the singularity but cannot reach it. In further developments the wormholes were compactified into *punctures* in the spacetime manifold, and then finally into *moving punctures*[67,68] and *trumpets*[69,70] that could be identified[71] as moving BHs. The calculations are done so that the grid points avoid puncture singularities. Allowing the punctures to move was the key step in making this method work.
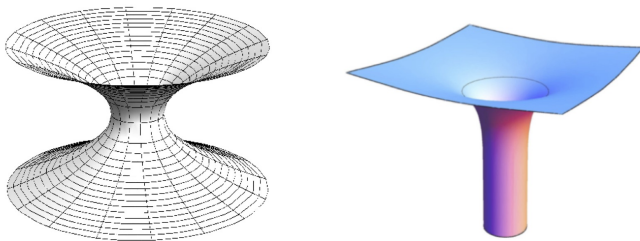

FIG. 5. Wormhole(left) and trumpet (right) representation of a BH. (From Refs. 69 and 70).

F. Meshes, Coordinates, Numerical Integration

The spatial extension of a BH–BH coalescence is huge. At the beginning, the BHs are widely separated and spacetime is essentially flat except near the BH horizons. Post-Newtonian physics holds sway. Just before coalescence, the BH's are only tens to hundreds of kilometers

apart, spacetime is highly curved and general relativity is dominant. Clearly, solving this problem involves wildly different length scales as it moves toward coalescence, with corresponding changes required in the numerical meshes. *Adaptive Mesh Refinement* schemes[72] have been developed to handle this issue.

The same consideration applies to the choice of coordinate system. For a BH–BH system, it is natural to choose one that has two spherical-polar centers in close, evolving into nearly spherical symmetry far away (see Fig. 4). In addition, much better numerical accuracy in satisfying the boundary conditions at the BH horizons will result if the coordinate lines are perpendicular to the BH horizon surface. We must also account for the motion of the BHs and the distortion of their horizons as the coalescence evolves. As Fig. 4 shows, this can lead to great numerical complexity and the clear need to use *curvilinear* coordinates and *non-rectangular* mesh schemes.

The numerical integration procedures in most common use are finite difference (FD)[73] or spectral interpolation (Spec)[74–76] methods. Both have long, well-known histories. FD methods yield approximate solutions to PDEs at specific points on the mesh. Spectral methods utilize smooth functions fitted to several mesh points that can provide highly accurate values at any location.

G. Numerical calculations of BH–BH coalescence

The pioneering Hahn–Lindquist computation treated two equal-mass BHs that were represented by a manifold containing co-joined wormholes described by Einstein–Rosen bridges. A dozen years later, Smarr and collaborators[77] used a similar model to study the head-on collision of non-rotating BH's with emission of gravitational radiation.

While neither of these calculations converged to a finite result, at the time there appeared to be no fundamental obstacle to achieving realistic results once enough computational power could be brought to bear. The stability issues mentioned in Sec. IV B, especially regarding hyperbolicity, maintaining constraints, and how best to handle the physical BH singularities were not yet fully appreciated. Dealing with these issues awaited the arrival of BSSNOK (*ca.* 1998), GCHD (2005) and the "moving punctures" (2005) algorithms.

In 2005, great breakthroughs were achieved by Pretorius[57] and the Brownsville[67] and Goddard[68] groups. Working independently and using quite different methods, they performed stable, accurate simulations of BH–BH coalescence that agreed very well with each other.[78] Fig. 6 compares their calculated polarizations for a head-on collision of equal-mass BHs resulting in the formation of a Kerr BH. Pretorius[57] used the GHCD formulation and BH excision. The Brownsville[67] and Goddard[68] groups used the BSSNOK formulation with the BHs represented by moving punctures. These early calculations all employed FD integration methods.

It's not possible to overstate the importance of these

results. With reliable, highly accurate numerical methods in hand, not only is the full scientific content of the gravity-wave detections revealed, but more realistic calculations are possible (*e.g.* including unequal BH masses, spin effects and eccentric orbits). Detailed calculations of more complicated gravitational systems, such as NS binaries[79] or NS–BH systems, as well as detailed tests of strong-field general relativity,[80] have begun. Many codes are available; most use a BSSNOK+FD framework, the others a GHCD+Spec treatment.[81]
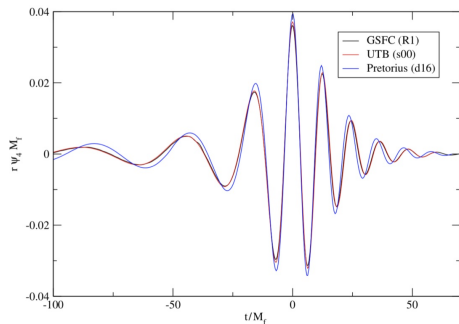

FIG. 6. Comparison of calculations from Pretorius[57] (red), Campanelli *et al.*[67] (blue) and Centrella *et al.*[68] (black). The abscissa shows time (in units of the final BH mass) and the ordinate is the + polarization of the outgoing gravitational radiation. (From Ref. 78)

H.   Inspiral – Merger – Ringdown (IMR) models

To identify possible BH–BH mergers and obtain estimates of their physical parameters, the data analyses use "template banks" of strain waveforms that can be matched in real time with incoming strain data.

However, assembling a template bank is a major challenge. Because templates can depend on as many as 17 parameters, thousands to millions of them are needed. Since each fully-NR calculation takes weeks to months to do, this is a totally impractical goal. Existing fully relativistic waveform catalogs[82] contain at most a few thousand templates.

Instead, since most of the strain waveform (inspiral to just before merger and the ringdown afterwards) can be accurately modeled using highly efficient post-Newtonian,[6] EOB[7] and quasi-normal mode[12] methods (*i.e.* without the numerical relativity portion), we can normalize the EOB or PN parts against existing numerical relativity catalogs to obtain a robust, highly efficient surrogate for the full calculation. These approaches[83–85]

are called *IMR models* and are in wide use. For parameter extraction this works very well because many of them (*e.g.* BH spins, polarizations and orbit eccentricity) are largely determined by the inspiral part of the waveform, before numerical relativity is necessary. This would not be true for tests of strong-field general relativity.

I.   You can try this at home

Should you wish to do calculations on your own, there are very helpful resources available: consult the *Simulating Extreme Spacetimes (SXS)*,[86] *Einstein Toolkit*[87] and *Super Efficient Numerical Relativity (SENR)*[76,88] websites for more information. Refs. 35–37 also offer numerical examples. The LIGO Open Science Center[89] provides data from gravitational-wave observations along with access to tutorials and software tools. You can also participate in the LIGO search for gravitational waves by signing up with Einstein@Home.[90]

V.   FINAL COMMENT

GW150914 was a supernova in the history of physics and cosmology. It, and the LIGO/VIRGO discoveries since then, have amazed even the most optimistic among us. GW170817, the first-ever sighting of a NS–NS merger and its subsequent electromagnetic counterparts, has provided a remarkable glimpse of the power of multi-messenger astronomy. The last three years have revealed just how much the "gravitational Universe" has to teach us now that we can see it.

It has taken 100 years to reach this point. Because of the genius of Albert Einstein, who saw that the geometry of the Universe was more subtle than realized by Isaac Newton, and the incredible ingenuity of the engineers and scientists of the gravitational science community, we can now use gravitational waves as a tool to decode the Universe. But without the generosity and patience of our fellow citizen-scientists the world over, these discoveries would not have been possible.

[*] reisenst@mit.edu

[1] D. Martynov, *et al.* "The Sensitivity of the Advanced LIGO Detectors at the Beginning of Gravitational Wave Astronomy", Phys. Rev. D**93**, 1102004 (2016).

[2] B. P. Abbott, *et al.* (LIGO Scientific Collaboration and Virgo Collaboration), "Observation of Gravita-

tional Waves from a Binary Black Hole Merger", Phys. Rev. Lett. **116**, 061102 (2016), doi: 10.1103/PhysRevLett.116.061102.

[3] B.P. Abbott, *et al.* (LIGO Scientific Collaboration and Virgo Collaboration), "Properties of the Binary Black Hole Merger GW150914", arXiv: 1602.03840 [gr-qc].

[4] B. P. Abbott, *et al.* (LIGO Scientific Collaboration and Virgo Collaboration), "Observing gravitational-wave transient GW150914 with minimal assumptions", Phys. Rev. D**93**, 122004 (2016).

[5] B.P. Abbott, *et al.* (LIGO Scientific Collaboration and Virgo Collaboration), "GW150914: First results from the search for binary black hole coalescence with Advanced LIGO", Phys. Rev. D**93**, 122003 (2016).

[6] E. Poisson and C. M. Will, *Gravity: Newtonian, Post-Newtonian, Relativistic,* (Cambridge U.P., Cambridge, 2014).

[7] T. Damour and A. Nagar, "The Effective One-Body description of the Two-Body Problem", in *Astrophysical Black Holes,* edited by F. Haardt *et al.,* Lecture Notes in Physics **905**, (Springer, Heidelberg, 2016).

[8] B. P. Abbott, *et al.* (LIGO Scientific Collaboration and Virgo Collaboration), "Directly comparing GW150914 with numerical solutions of Einstein's equations for binary black hole coalescence", Phys. Rev. D**94**, 064035 (2016).

[9] G. Lovelace, *et al.,* "Modeling the source of GW150914 with targeted numerical-relativity simulations", Class. Quant. Grav." **33**, 244002 (2016).

[10] A. R. Williamson, *et al.* "Systematic challenges for future gravitational wave measurements of precessing binary black holes", arXiv:1709.03095 [gr-qc].

[11] S. A. Teukolsky, "The Kerr Metric", arXiv:1410.2130v2 [gr-qc].

[12] T. Damour and A. Nagar, "New analytic representation of the ringdown waveform of coalescing spinning black hole binaries", Phys. Rev. D **90**, 024054 (2014).

[13] The LIGO Scientific Collaboration and the Virgo Collaboration, "The basic physics of the binary black hole merger GW150914", Ann. Phys. (Berlin) **529**, 1600209 (2017).

[14] R. J. A. Lambourne, *Relativity, Gravitation and Cosmology,* (Cambridge U.P., Cambridge, 2010).

[15] J. B. Hartle, *Gravity: An Introduction to Einstein's General Relativity,* 3rd ed. (Addison-Wesley, San Francisco, 2003).

[16] A Riemann manifold is a curved space which is locally flat near each spacetime point. The Riemann curvature tensor describes the curvature by measuring the change of a vector as it is transported around a closed path on a manifold, while always remaining parallel to its original orientation. This is referred to as "parallel transport."

[17] For a brief overview see M. R. Dennis, "Tensors and Manifolds", in *The Princeton Companion to Applied Mathematics,* edited by N. J. Higham *et al.,* (Princeton U.P., Princeton, 2015) pp. 127–130.

[18] For a brief overview see: M. A. H. MacCallum, "Einstein's Field Equations", in Ref. 17, pp. 144–146.

[19] Einstein's equations are often written using units in which the speed of light (c) and Newton's gravitational constant (G) are set equal to 1. Thus 1 $M_\odot$ is equivalent to $\sim 1.5 km$ or to $\sim 5 \mu s$.

[20] The Einstein tensor measures the curvature of the manifold in a region near each point.

[21] The Ricci tensor provides a measure of the difference in geometry between a given Riemann metric and ordinary Euclidean n–space.

[22] The Ricci scalar is a real number that measures the intrinsic geometry of a Riemann manifold near a given point.

[23] Minkowski space is described by a flat 4-dimensional manifold in which the time coordinate is treated differently than the three space coordinates. Thus Minkowski space, though flat, is not a 4-dimensional Euclidean space.

[24] Ø. Grøn, "Celebrating the centenary of the Schwarzschild solutions", Am. J. Phys. **84**, 537–541 (2016).

[25] C. W. Misner, K. S. Thorne and J. A. Wheeler, *Gravitation,* (Princeton U.P., Princeton, 2017) pp 875-876.

[26] É. É. Flanagan and S. A. Hughes, "The basics of gravitational wave theory", New J. Phys. **7**, 204–258 (2005).

[27] J. D. E. Creighton and W. G. Anderson, *Gravitational-Wave Physics and Astronomy,* Wiley Series in Cosmology (Wiley-VCH, Weinheim, 2011), pp. 135-6.

[28] Gravitational waves are ripples in spacetime itself rather than a disturbance superimposed on it (*e.g.* emission of an electromagnetic wave from a vibrating charge). Since there is no physical mechanism to absorb them, gravitational waves can travel cosmological distances at speed c without dispersion. This has been confirmed recently in Ref. 29 to about 1 part in 10^{15}.

[29] B. P. Abbott, *et al.* (LIGO Scientific Collaboration and Virgo Collaboration, Fermi Gamma-ray Burst Monitor, and INTEGRAL), "Gravitational Waves and Gamma-Rays from a Binary Neutron Star Merger:GW170817 and GRB 170817A", ApJ. Lett. **838**:L13, 1-27 (2018).

[30] An essential difference is that the lowest order of electromagnetic radiation is the dipole term, while for gravitational radiation it is the quadrupole. So any source of gravitational waves must possess mass distributions with time-varying quadrupole and/or higher multipole moments.

[31] Ref. 25, p. 444.

[32] N. Bahcall, "Hubble's law and the expanding Universe", Proc. Natl. Acad. Sci. **112**, 3173–3175 (2015).

[33] F. E. Bloom,"Breakthrough of the Year", *Science Magazine,* **282**, Issue 5397 (1998).

[34] I. Hawke, "Numerical Relativity", in Ref. 17, pp. 680–687.

[35] T. W. Baumgarte and S. L. Shapiro, *Numerical Relativity: Solving Einstein's Equations on the Computer,* (Cambridge U.P., Cambridge, 2010).

[36] M. Alcubierre, *Introduction to 3+1 Numerical Relativity,* International Series of Monographs on Physics **140** (Oxford U. P., Oxford, 2012).

[37] É. Gourgoulhon, *3+1 Formalism in General Relativity,* Lecture Notes in Physics **846** (Springer Heidelberg, 2012).

[38] J. Centrella, J. G. Baker, B. J. Kelly and J. R. van Meter, "Black-hole binaries, gravitational waves, and numerical relativity", Rev. Mod. Phys. 82:3069 (2010).

[39] Y. Fourès-Bruhat, "Thèoréme d'existence pour certain systémes d'equations aux dérivées partielles non-linéaires", Acta Math. **88**, 141–225 (1952).

[40] See Ref. 38, Section II-B, and also V. Cardoso, L. Gualtieri, C. Herdeiro and U. Sperhake, "Exploring New Physics Frontiers Through Numerical Relativity", Living Rev. Relativity **18**, 1-156 (2015) pp. 9-14.

[41] R. Arnowitt, S. Deser and C. W. Misner, "The Dynamics of General Relativity", in *Gravitation: an introduction to current research,* edited by L. Witten (Wiley, New York, 1962). Reprinted as arXiv:0405109v1 [gr-qc].

[42] J. W. York, "Kinematics and Dynamics of General Relativity", in *Sources of Gravitational Radiation,* edited by L.

Smarr (Cambridge U.P., Cambridge, 1979) pp. 83–126.

[43] Ref. 36, Ch. 2, p. 75.

[44] Gauge freedom allows modification of physical equations to improve solubility as long as the physical observables don't change. Since these cannot depend on the coordinate system used, changing from one to another is an example of gauge freedom. Another[27] is the use of scalar and vector potential functions ϕ and $\mathbf{A}$ in Maxwell's equations.

[45] $\mathcal{K}_{ij}$ measures the change in direction of a surface normal vector under parallel transport (Ref. 36 p. 69).

[46] D. Hilditch, " An Introduction to Well-Posedness and Free-Evolution", arXiv:1308.2012v1 [gr-qc].

[47] I thank F. Tabakin for pointing this out.

[48] Ref. 35, Ch. 11.

[49] Ref. 36, Ch. 5.

[50] P. Fromholz, E. Poisson and C. M. Will, "The Schwarzschild metric: It's the coordinates, stupid!", Amer. J. Phys. **82**, 295-300 (2014).

[51] T. Nakamura, K. Oohara and Y. Kojima, "General relativistic collapse to black holes and gravitational waves from black holes", Prog. Theor. Phys. Suppl. **90**, 1–218 (1987).

[52] M. Shibata and T. Nakamura, "Evolution of three-dimensional gravitational waves: Harmonic slicing case," Phys. Rev. **52**, 5428–5444 (1995).

[53] T. W. Baumgarte and S. L. Shapiro, "Numerical integration of Einstein's field equations", Phys. Rev. D **59**, 024007 (1998).

[54] Ref. 36, p. 81.

[55] D. Garfinkle, "Harmonic coordinate method for simulating generic singularities", Phys. Rev. D **65**, 044029 (2002).

[56] F. Pretorius, "Binary Black Hole Coalescence", arXiv:0710.1338v1 [gr-qc].

[57] F. Pretorius, "The Evolution of Binary Black-Hole Spacetimes", Phys. Rev. Lett. **95**, 121101 (2005).

[58] H. P. Pfeiffer, "The initial value problem in numerical relativity," arXiv:0412002v1 [gr-qc].

[59] G. B. Cook, "Initial Data for Numerical Relativity," Living Rev. Relativ. (2000) 3:5.

[60] Ref. 35, Chs. 3, 12, 15.

[61] Ref. 36, Ch. 3.

[62] Ref.15, Chapter 15, p. 310.

[63] See M. Alcubierre and B. Brugmann, "Simple excision of a black hole in 3+1 numerical relativity", Phys. Rev. D **63**, 104006 (2001).

[64] A. Einstein and N. Rosen, "The Particle Problem in the General Theory of Relativity", Phys. Rev. **48**, 73–77 (1935).

[65] S. G. Hahn and R. W. Lindquist, "Two-body Problem in Geometrodynamics", Ann. Phys. **29**, 304–331 (1964).

[66] The term "Black Hole" was not coined by John Wheeler until 1967.

[67] M. Campanelli, C. O. Lousto, P. Marronetti, and Y. Zlochower, *"Accurate Evolutions of Orbiting Black-hole binaries without Excision",* Phys. Rev. Lett. **96**, 111101 (2006).

[68] J. G. Baker, J. Centrella, D. Choi, M. Koppitz and J. van Meter, "Gravitational-Wave Extraction from an Inspiraling Configuration of Merging Black Holes", Phys. Rev. Lett. **96**, 111102 (2006).

[69] M. Hannam, *et al.*, "Wormholes and trumpets: Schwarzschild spacetime for the moving puncture generation", Phys. Rev. D **78**, 064020 (2008), doi:10.1103/PhysRevD.78.064020.

[70] K. A. Dennison and T. W. Baumgarte, "A Simple Family of Analytical Trumpet Slices of the Schwarzschild Space-time", Class. Quantum Grav. **31** (2014) 117001, doi: 10.1088/0264-9381/31/11/117001.

[71] J. Thornburg, *et al.*, "Are moving punctures equivalent to black holes?", arXiv:0701038v2 [gr-qc].

[72] K. Clough, *et al.*, "GRChombo: Numerical Relativity with Adaptive Mesh Refinement", arXiv:[1503.03436v3 [gr-qc].

[73] M. W. Choptuik, "Relativistic Astrophysics and Numerical Relativity: Numerical Analysis for Numerical Relativists", *VII Mexican School on Gravitation and Mathematical Physics 2006,* Journal of Physics: Conference Series Vol. **91** (Institute of Physics, Bristol, 2006).

[74] L. E. Kidder and L. S. Finn, "Spectral methods for numerical relativity: The initial data problem", Phys. Rev. D **62**, 084026 (2000).

[75] J. P. Boyd, *Chebyshev and Fourier Spectral Methods*, Second Ed. (Dover Publications, New York, 2000).

[76] I. Ruchlin, Z. B. Etienne and T. W. Baumgarte, "SENR/NRPy+: Numerical Relativity in Singular Curvilinear Coordinate Systems", arXiv:1712.07658v1 [gr-qc].

[77] L. Smarr, A. Čadež, B. DeWitt and K. Eppley, "Collision of two black holes: Theoretical framework", Phys. Rev. **14**, 2443–2452 (1976).

[78] J. G. Baker, M. Campanelli, F. Pretorius and Y. Zlochower, "Comparisons of binary black hole merger waveforms", Class. Quant. Grav. **24** (2007) S25-S31, doi: 10.1088/0264-9381/24/12S03.

[79] B. P. Abbott, *et al.* (LIGO Scientific Collaboration and Virgo Collaboration), "GW170817: Observation of Gravitational Waves from a Binary Neutron Star Inspiral", Phys. Rev. Lett. **119**, 161101 (2017).

[80] B. P. Abbott, *et al.* (LIGO Scientific Collaboration and Virgo Collaboration), "Tests of General Relativity with GW150914", Phys. Rev. Lett. **116**, 221101 (2016).

[81] H. Pfeiffer, "Numerical simulations of compact object binaries," Class. Quantum Grav. **29**, 124004 (2012) p. 3, and J. Aasi, *et al.*, "The NINJA-2 Project: detecting and characterizing gravitational waveforms modeled using numerical binary black hole simulations", arXiv:1401:0939v1.

[82] A. H. Mroué, *et al.,* "Catalog of 174 Binary Black Hole Simulations for Gravitational Wave Astronomy," Phys. Rev. Lett. **111**, 241104 (2013) and K. Jani, *et al.,* "Georgia Tech Catalog of Gravitational Waveforms", arXiv:1605.03204v1 [gr-qc].

[83] A. Bohé, *et al.*, "An improved effective-one-body model of spinning, nonprecessing binary black holes for the era of gravitational-wave astrophysics with advanced detectors", Phys. Rev. D **95**, 044028 (2017).

[84] S. Khan, *et al.*, "Frequency-domain gravitational waves from nonprecessing black-hole binaries. II. A phenomenological model for the advanced detector era", Phys. Rev. D **93**, 044007 (2016).

[85] M. Hannam, *et al.*, "A simple model of complete precessing black-hole-binary gravitational waveforms", arXiv:1308.3271 [gr-qc].

[86] Simulating Extreme Spacetimes website: <https://www.black-holes.org>.

[87] Einstein Toolkit website: <https://einsteintoolkit.org>.

[88] Super Efficient Numerical Relativity (SENR) website: <https://math.wvu.edu/ zetienne/SENR/index.html>. Also see Ref. 76.

[89] https://losc.ligo.org/about/

[90] Einstein@Home website: <https://www.einsteinathome.org>.